

Extended Lubrication Theory: Estimation of Fluid Flow in Channels with Variable Geometry

Behrouz Tavakol and Douglas P. Holmes

Department of Engineering Science & Mechanics, Virginia Tech, Blacksburg, VA 24061

Guillaume Froehlicher and Howard A. Stone*

Department of Mechanical & Aerospace Engineering, Princeton University, Princeton, NJ 08544

(Dated: March 11, 2014)

Lubrication theory is broadly applicable to the flow characterization of thin fluid films and the motion of particles near surfaces. We offer an extension to lubrication theory by considering higher-order terms of the analytical approximation to describe the fluid flow in a channel with features of a modest aspect ratio. We find good agreement between our analytical results and numerical simulations. We show that the extended lubrication theory is a robust tool for an accurate estimate of laminar fluid flow in channels with features on the order of the channel height, accounting for both smooth and sharp changes in geometry.

I. INTRODUCTION

Lubrication theory is an approximation to the Navier-Stokes and continuity equations at low Reynolds numbers for narrow geometries with slow changes in curvature [1–3]. The approach is used regularly to describe the velocity field and pressure gradient in fluid film lubricants [4, 5], the motion of particles within a fluid and near boundaries [6, 7], the fluid flow passing through a microchannel with a known geometry [8–11], flow driven by the contracting walls of a soft channel, *e.g.*, an insect’s trachea [12, 13], and the flow of thin liquid films with free-surfaces [14], *e.g.*, when a droplet wets a solid surface [15, 16]. Classical lubrication theory (CLT) is suitable for all above cases provided that the ratio of thickness to the axial length scale is on the order of $O(10^{-1})$ or less. Due to its simplicity and versatile applications, lubrication theory is applied widely.

In this study, we obtain higher-order terms of the lubrication approximation and present an extension to lubrication theory, which we refer to as extended lubrication theory (ELT), to address two limitations of CLT. First, the use of ELT is no longer limited to small gaps and thin films. Second, the boundaries can be described by any mathematical shape function with arbitrary curvatures as long as they are continuous and differentiable. In addition, we show how the differentiability condition may be relaxed at low Reynolds numbers by considering geometries that are piece-wise differentiable. We compare the results of different orders of the analytical solution with direct numerical solutions of the Navier-Stokes equation to define a threshold for considering higher-order terms in the solution.

II. THEORETICAL APPROXIMATION

We consider working to higher order in traditional lubrication theory to describe fluid flow in nonuniform channel shapes with modest aspect ratios. Thus, we consider incompressible, steady, two-dimensional pressure-driven flow in a channel with shape $y = h(x) = h_0 H(X)$, where $X = x/L_0$, L_0 is the channel length, h_0 is a characteristic channel height, $H(X)$ is a normalized shape function, and $\delta = h_0/L_0 \ll 1$. A typical geometry in the form of a constriction is shown in Fig. 1a. We assume that the Reynolds number is small and so consider the continuity and Stokes equations

$$\nabla \cdot \mathbf{u} = 0 \quad \text{and} \quad \mu \nabla^2 \mathbf{u} = \nabla p, \quad (1)$$

where $\mathbf{u} = (u, v)$ is the velocity field and μ is the fluid viscosity. We denote the constant flow rate (per unit width) as q_0 . Consistent with the traditional lubrication approximation we choose to introduce dimensionless variables according to

$$X = \frac{x}{L_0}, \quad Y = \frac{y}{h_0}, \quad U = \frac{u}{q_0/h_0}, \quad V = \frac{v}{q_0/L_0}, \quad P = \frac{p}{\Delta p} = \frac{p}{\mu q_0 L_0 / h_0^3}. \quad (2)$$

* hastone@princeton.edu

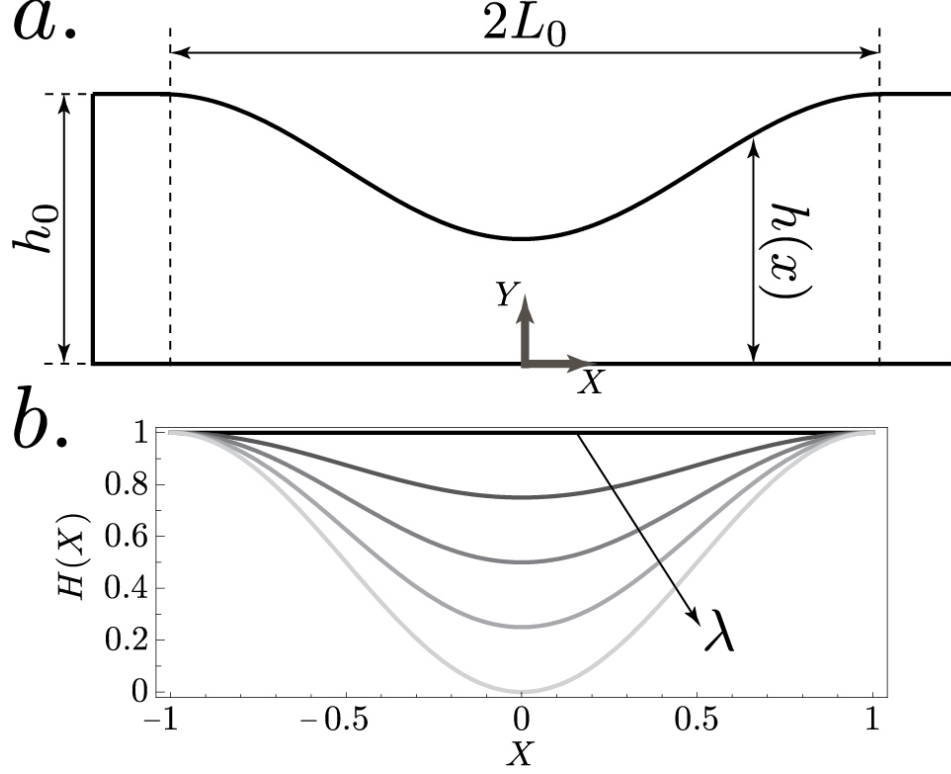


FIG. 1. (a) A schematic of the channel with shape $y = h(x) = h_0 H(x)$. (b) Shape function of $H(X) = 1 - \frac{\lambda}{2} (1 + \cos(\pi X))$ for different λ .

The dimensionless equations corresponding to (1) for a two-dimensional flow are

$$\frac{\partial U}{\partial X} + \frac{\partial V}{\partial Y} = 0 \quad (3a)$$

$$\delta^2 \frac{\partial^2 U}{\partial X^2} + \frac{\partial^2 U}{\partial Y^2} = \frac{\partial P}{\partial X} \quad (3b)$$

$$\delta^4 \frac{\partial^2 V}{\partial X^2} + \delta^2 \frac{\partial^2 V}{\partial Y^2} = \frac{\partial P}{\partial Y} \quad (3c)$$

These equations are to be solved with boundary conditions

$$U = 0, V = 0 \quad \text{at } Y = 0, H(X), \quad \text{and} \quad \int_0^{H(X)} U(X, Y) dY = 1, \quad (4)$$

where the integral constraint states that the total flow rate is prescribed. We will determine the corresponding pressure drop across the constriction such that the pressure gradient tends to a constant as $X \rightarrow \pm 1$. Note that the problem statement only involves one dimensionless parameter δ^2 .

A. Perturbation expansion and the leading-order result from lubrication theory

Our first steps follow standard discussions in textbooks, e.g. Leal [2]. Because the problem statement only involves δ^2 , which is assumed to be small, we seek a solution to (3) of the form

$$U(X, Y; \delta) = U_0(X, Y) + \delta^2 U_2(X, Y) + \delta^4 U_4(X, Y) + \dots \quad (5a)$$

$$V(X, Y; \delta) = V_0(X, Y) + \delta^2 V_2(X, Y) + \delta^4 V_4(X, Y) + \dots \quad (5b)$$

$$P(X, Y; \delta) = P_0(X, Y) + \delta^2 P_2(X, Y) + \delta^4 P_4(X, Y) + \dots \quad (5c)$$

At leading order, we have the familiar classical lubrication problem

$$\frac{\partial U_0}{\partial X} + \frac{\partial V_0}{\partial Y} = 0 \quad (6a)$$

$$\frac{\partial^2 U_0}{\partial Y^2} = \frac{\partial P_0}{\partial X} \quad (6b)$$

$$\frac{\partial P_0}{\partial Y} = 0, \quad (6c)$$

with $U_0 = 0$ at $Y = 0$ and $H(X)$. The solution is

$$U_0(X, Y) = \frac{1}{2} \frac{dP_0}{dX} (Y^2 - YH(X)) \quad (7)$$

and the pressure gradient, which only depends on X , follows from applying the integral constraint $\left(\int_0^{H(X)} U_0(X, Y) dY = 1\right)$

$$\frac{dP_0}{dX} = -\frac{12}{H(X)^3}. \quad (8)$$

The corresponding velocity distribution is then

$$U_0(X, Y) = \frac{6}{H(X)^3} (YH(X) - Y^2). \quad (9)$$

To provide an example, we consider the shape function

$$H(X) = 1 - \frac{\lambda}{2} (1 + \cos(\pi X)) \quad (1 > \lambda \geq 0), \quad (10)$$

as sketched in Fig. 1b. The leading-order pressure drop ΔP_0 is then calculated to be (the integration was accomplished with Mathematica)

$$P_0(-1) - P_0(1) = \Delta P_0 = -\int_{-1}^1 \frac{dP_0}{dX} dX = 12 \int_{-1}^1 \frac{1}{\left(1 - \frac{\lambda}{2} - \frac{\lambda}{2} \cos(\pi X)\right)^3} dX = \frac{3(3\lambda^2 - 8\lambda + 8)}{(1 - \lambda)^{5/2}}. \quad (11)$$

Before proceeding further, we determine the velocity component $V_0(X, Y)$ using the continuity equation. Although equation (6a) is first order in Y , we expect it to satisfy two boundary conditions, as $V_0(X, 0) = V_0(X, H(X)) = 0$. Using the continuity equation, and imposing $V_0(X, 0) = 0$, we have

$$V_0(X, Y) = -\int_0^Y \frac{\partial U_0(X, S)}{\partial X} dS, \quad (12)$$

which yields

$$V_0(X, Y) = 2Y^3 (H^{-3})' - 3Y^2 (H^{-2})', \quad (13)$$

where primes denotes X derivatives. We then note that at $Y = H(X)$ direct differentiation shows that (13) yields $V_0(X, H(X)) = 0$. Alternatively, we can write

$$V_0(X, H(X)) = -\int_0^{H(X)} \frac{\partial U_0}{\partial X} dY = -\frac{d}{dX} \int_0^{H(X)} U_0 dY + U_0(X, H(X)) \frac{dH}{dX} = 0, \quad (14)$$

as the second term on the right-hand side vanishes owing to the no-slip condition and the first term on the right-hand side vanishes since the flow rate is constant. The same idea applies for evaluating the Y -component of velocity at every order in the analysis below and the no-slip boundary condition is satisfied for both velocity components of \mathbf{u} .

B. The $\mathcal{O}(\delta^2)$ term in the perturbation expansion

In most calculations utilizing lubrication theory the development is truncated with the leading-order term calculated in the preceding section. Here our interest is to improve the approximation by including additional terms in the perturbation solution. At the next order, $\mathcal{O}(\delta^2)$, the perturbation expansion yields

$$\frac{\partial U_2}{\partial X} + \frac{\partial V_2}{\partial Y} = 0 \quad (15a)$$

$$\frac{\partial^2 U_2}{\partial Y^2} - \frac{\partial P_2}{\partial X} = -\frac{\partial^2 U_0}{\partial X^2} \quad (15b)$$

$$\frac{\partial P_2}{\partial Y} = \frac{\partial^2 V_0}{\partial Y^2}, \quad (15c)$$

with boundary conditions $U_2 = 0$ at $Y = 0$ and $H(X)$, and $\int_0^{H(X)} U_2(X, Y) dY = 0$. This last integral constraint follows since all of the fluid flux is specified in the scaling used to establish the leading-order problem. We seek the velocity distribution and pressure drop $\Delta P_2 = P_2(-1) - P_2(1)$ needed to enforce the constraint on the flux.

We can integrate the last equation of (15), and use continuity, to obtain

$$P_2(X, Y) = -\frac{\partial U_0}{\partial X} + c_3(X), \quad (16)$$

where the function $c_3(X)$ is allowed by the integration. With this pressure distribution, we use the X -momentum equation to find

$$\frac{\partial^2 U_2}{\partial Y^2} = \frac{dc_3}{dX} - 2\frac{\partial^2 U_0}{\partial X^2} \quad (17)$$

where U_0 is given by equation (9). Upon integration, and application of the boundary conditions, we find

$$U_2(X, Y) = -2(H(X)^{-2})''(Y^3 - H(X)^2 Y) + (H(X)^{-3})''(Y^4 - H(X)^3 Y) + \frac{1}{2}\frac{dc_3}{dX}(Y^2 - H(X)Y). \quad (18)$$

Since we have accounted for the specified dimensionless flow rate at leading order, then we now require $\int_0^{H(X)} U_2(X, Y) dY = 0$, which leads to

$$\frac{dc_3}{dX} = 6(H(X)^{-2})''H(X) - \frac{18}{5}(H(X)^{-3})''H(X)^2. \quad (19)$$

Equations (18) and (19) give the second-order X -component of the velocity $U_2(X, Y)$ for any shape function $H(X)$. Integrating (16), taking into account that $\frac{\partial U_0}{\partial X}$ vanishes as $X \rightarrow -1$ and 1 , and using (19), we obtain the pressure drop ΔP_2 at this order as

$$P_2(-1) - P_2(1) = \Delta P_2 = -\int_{-1}^1 \frac{\partial P_2}{\partial X} dX = -\int_{-1}^1 \frac{dc_3}{dX} dX = \frac{12\pi^2\lambda^2}{5(1-\lambda)^{3/2}}, \quad (20)$$

where again we have evaluated the integral for the shape function (10).

We determine $V_2(X, Y)$ using the continuity equation and imposing $V_2(X, 0) = 0$, which leads to the rather messy expression

$$\begin{aligned} V_2(X, Y) = & (H(X)^{-2})''' \left(\frac{1}{2}Y^4 - H(X)^2 Y^2 \right) - 2(H(X)^{-2})'' H'(X) Y^2 - \frac{d^2 c_3}{dX^2} \left(\frac{1}{6}Y^3 - \frac{1}{4}HY^2 \right) \\ & - (H(X)^{-3})''' \left(\frac{1}{5}Y^5 - H(X)^3 Y^2 \right) + \frac{3}{2}(H(X)^{-3})'' (H'(X))^2 Y^2 + \frac{1}{4}\frac{dc_3}{dX} H'(X) Y^2. \end{aligned} \quad (21)$$

This equation only involves the shape function $H(X)$, since $\frac{dc_3}{dX}$ is given in (19). As in the previous section, it can be verified that $V_2(X, H(X)) = 0$.

C. The perturbation expansion at $\mathcal{O}(\delta^4)$

It is useful to go one step further simply to illustrate that the basic analytical steps carry through at every order. The higher-order terms help to provide a better representation of flows in geometries with more rapid shape variations. We can continue these basic steps at $\mathcal{O}(\delta^4)$, where we have the equations

$$\frac{\partial U_4}{\partial X} + \frac{\partial V_4}{\partial Y} = 0 \quad (22a)$$

$$\frac{\partial^2 U_4}{\partial Y^2} - \frac{\partial P_4}{\partial X} = -\frac{\partial^2 U_2}{\partial X^2} \quad (22b)$$

$$\frac{\partial P_4}{\partial Y} = \frac{\partial^2 V_2}{\partial Y^2} + \frac{\partial^2 V_0}{\partial X^2}, \quad (22c)$$

with $U_4 = 0$ at $Y = 0$ and $H(X)$, and $\int_0^{H(X)} U_4(X, Y) dY = 0$. Using the results obtained above, these equations can be solved, though the algebraic manipulations involved become progressively more cumbersome. We outline the main steps below. First, the Y -momentum equation can be integrated, which, after using the continuity equation, yields

$$P_4(X, Y) = -\frac{\partial U_2}{\partial X} + \frac{\partial^2}{\partial X^2} \int_0^Y V_0(X, S) dS + c_5(X). \quad (23)$$

Second, from the X -momentum equation we have

$$\frac{\partial^2 U_4}{\partial Y^2} = -2\frac{\partial^2 U_2}{\partial X^2} + \frac{\partial^3}{\partial X^3} \int_0^Y V_0(X, S) dS + \frac{dc_5}{dX}. \quad (24)$$

Since $U_2(X, Y)$ is known from equation (18), then we calculate

$$\begin{aligned} \frac{\partial^2 U_2}{\partial X^2} &= (H^{-3})'''' Y^4 - 2(H^{-2})'''' Y^3 + \left[-\left(H^3 (H^{-3})'' \right)'' + 2\left(H^2 (H^{-2})'' \right)'' \right] Y \\ &\quad + \frac{1}{2} \frac{d^3 c_3}{dX^3} Y^2 - \frac{1}{2} \left(H \frac{dc_3}{dX} \right)'' Y. \end{aligned} \quad (25)$$

Combining the last two results, we find

$$\begin{aligned} \frac{\partial^2 U_4}{\partial Y^2} &= -\frac{3}{2} (H^{-3})'''' Y^4 + 3(H^{-2})'''' Y^3 + \left[2\left(H^3 (H^{-3})'' \right)'' - 4\left(H^2 (H^{-2})'' \right)'' \right] Y \\ &\quad - \frac{d^3 c_3}{dX^3} Y^2 + \left(H \frac{dc_3}{dX} \right)'' Y + \frac{dc_5}{dX}. \end{aligned} \quad (26)$$

It is straightforward to integrate twice and apply $U_4 = 0$ at $Y = 0$ and $H(X)$ to arrive at

$$\begin{aligned} U_4(X, Y) &= -\frac{1}{20} (H^{-3})'''' (Y^6 - H^5 Y) + \frac{3}{20} (H^{-2})'''' (Y^5 - H^4 Y) \\ &\quad + \frac{1}{3} \left[\left(H^3 (H^{-3})'' \right)'' - 2\left(H^2 (H^{-2})'' \right)'' \right] (Y^3 - H^2 Y) \\ &\quad - \frac{1}{12} \frac{d^3 c_3}{dX^3} (Y^4 - H^3 Y) + \frac{1}{6} \left(H \frac{dc_3}{dX} \right)'' (Y^3 - H^2 Y) + \frac{1}{2} \frac{dc_5}{dX} (Y^2 - HY). \end{aligned} \quad (27)$$

Since $\int_0^{H(X)} U_4(X, Y) dY = 0$, we obtain $\frac{dc_5}{dX}$

$$\begin{aligned} \frac{dc_5}{dX} &= \frac{3}{14} (H^{-3})'''' H^4 - \frac{3}{5} (H^{-2})'''' H^3 - \left[\left(H^3 (H^{-3})'' \right)'' - 2\left(H^2 (H^{-2})'' \right)'' \right] H \\ &\quad + \frac{3}{10} \frac{d^3 c_3}{dX^3} H^2 - \frac{1}{2} \left(H \frac{dc_3}{dX} \right)'' H. \end{aligned} \quad (28)$$

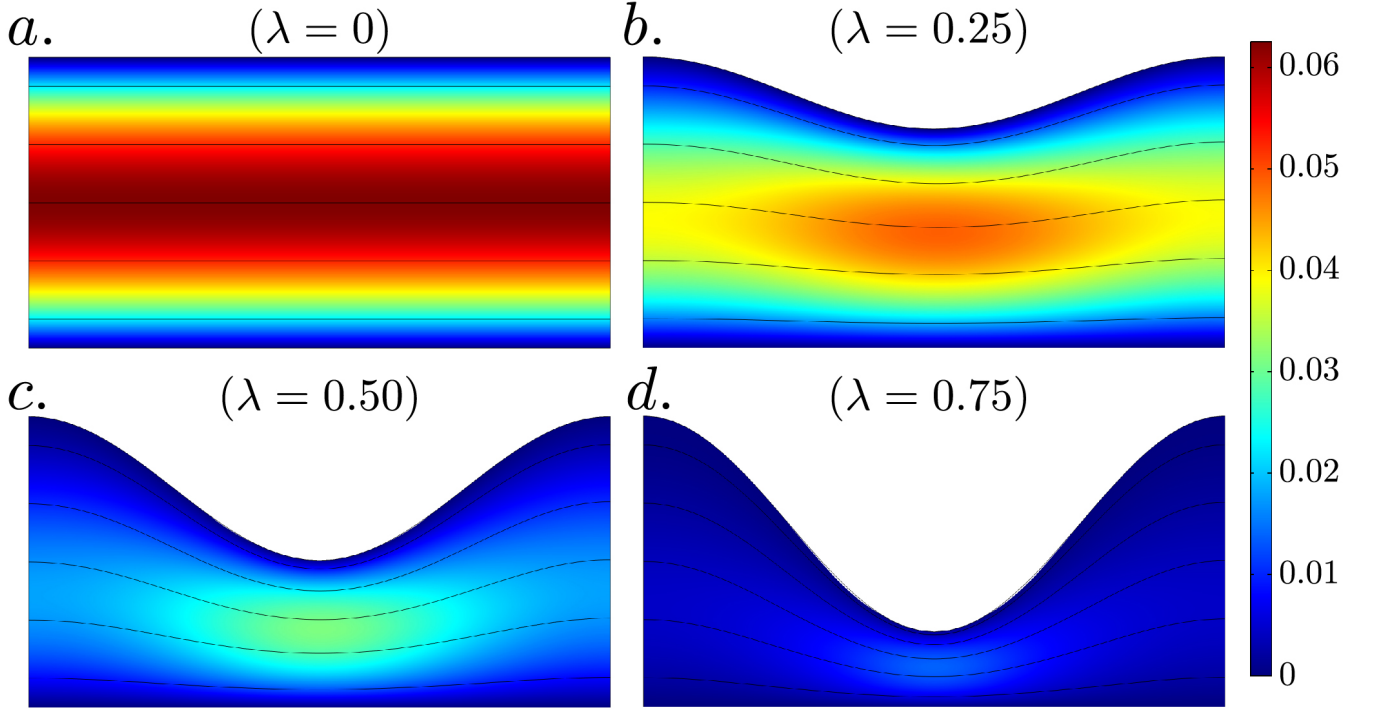


FIG. 2. Velocity magnitude obtained using numerical simulation for $\mathcal{Re} = 1$, $\delta = 1$, and λ varied from 0 to 1 (a-d).

The equations (18), (27), and (28) give the X -component velocity at this order for any choice of the shape function $H(X)$. We determine the correction to the pressure drop as

$$\begin{aligned}
 P_4(-1) - P_4(1) = \Delta P_4 &= - \int_{-1}^1 \frac{\partial P_4}{\partial X} dX = - \int_{-1}^1 \frac{dc_5}{dX} dX \\
 &= \frac{8\pi^4 (-428 (-1 + \sqrt{1-\lambda}) + 214 (-2 + \sqrt{1-\lambda}) \lambda + 53\lambda^2)}{175\sqrt{1-\lambda}}, \quad (29)
 \end{aligned}$$

where we have used Mathematica to accomplish the final integration for the shape function (10).

For a given flow rate (q_0), we have determined the dimensionless pressure drop $\Delta P = (\Delta P_{\text{applied}}) / (\mu q_0 L_0 / h_0^3)$ as a function of δ , where $\Delta P_{\text{applied}}$ is the difference in pressure applied at the two ends of the channel. In particular, $\Delta P = \Delta P_0(\lambda) + \delta^2 \Delta P_2(\lambda) + \delta^4 \Delta P_4(\lambda) + \mathcal{O}(\delta^6)$, where λ is defined by the given shape function (10).

III. COMPARISON OF THEORY AND NUMERICAL SIMULATIONS

We numerically solved the Navier-Stokes equation in its full form for incompressible, steady two-dimensional flow using COMSOL 4.3. The same scalings and dimensionless parameters introduced in equation (2) were used to obtain the dimensionless continuity and Navier-Stokes equations

$$\begin{aligned}
 \frac{\partial U}{\partial X} + \frac{\partial V}{\partial Y} &= 0 \\
 \mathcal{Re} \delta \left(U \frac{\partial U}{\partial X} + V \frac{\partial U}{\partial Y} \right) &= - \frac{\partial P}{\partial X} + \delta^2 \frac{\partial^2 U}{\partial X^2} + \frac{\partial^2 U}{\partial Y^2} \\
 \mathcal{Re} \delta^3 \left(U \frac{\partial V}{\partial X} + V \frac{\partial V}{\partial Y} \right) &= - \frac{\partial P}{\partial Y} + \delta^4 \frac{\partial^2 V}{\partial X^2} + \delta^2 \frac{\partial^2 V}{\partial Y^2}, \quad (30)
 \end{aligned}$$

where $\mathcal{Re} = \rho q_0 / \mu$ is the Reynolds number, ρ is the fluid density, and μ is the fluid viscosity. In the lubrication literature, it is common to define the reduced Reynolds number, $\mathcal{Re}^* = \mathcal{Re} \delta$, which also appears in (30). We used the weak form of (30) as the governing equations for the numerical model (see the appendix for more information), which

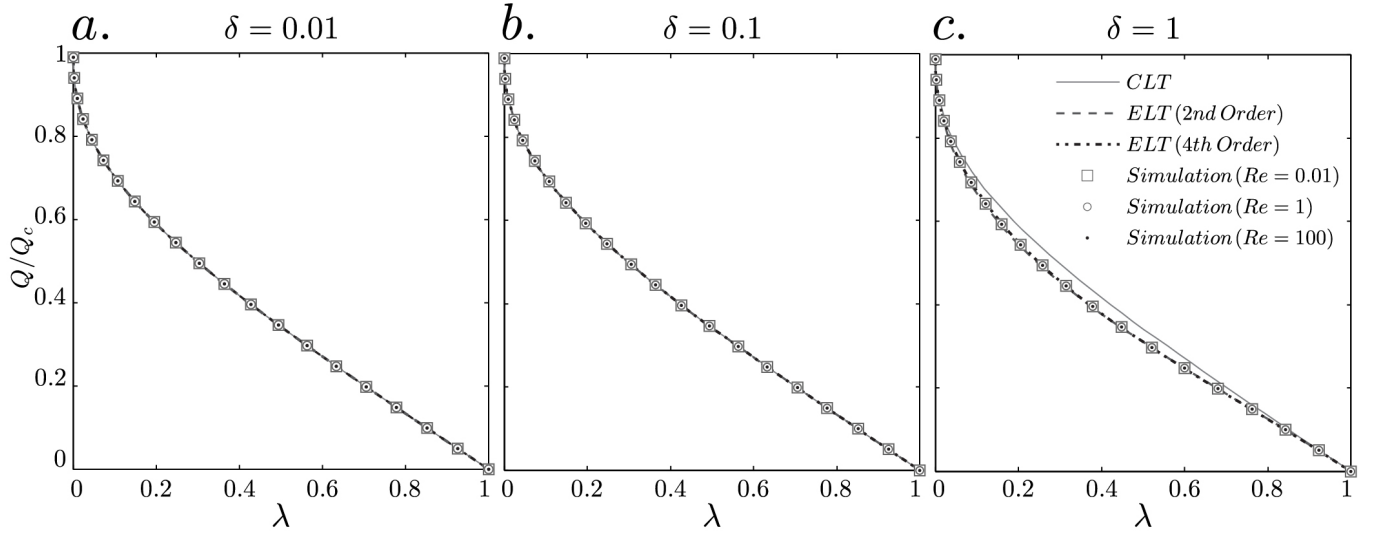


FIG. 3. Comparison between simulation results ($\mathcal{Re} = 100$ and $\delta = 0.01 - 1$) and different orders of analytical solutions. (a) $\delta = 0.01$. (b) $\delta = 0.1$. (c) $\delta = 1$.

depends on two dimensionless parameters: Reynolds number and the geometric variable, $\delta = h_0/L_0$. In addition, the shape function (10) adds another dimensionless parameter, λ , to this system.

Therefore, we performed the numerical simulations for a range of $\mathcal{Re} = 0.01 - 2000$ and $\delta = 0.01, 0.1$, and 1 while varying λ from 0 to 0.99 . The channel height was $H_0 = 1$ and a pressure drop of $\Delta P = 1$ was applied across the channel length. In this case the corresponding flow rate is evaluated from the simulation results. For example, simulation results for $\mathcal{Re} = 100$, $\delta = 1$, and different λ are shown in Fig. 2; notice that for the same pressure drop the magnitude of the velocity decreases systematically as the gap in the constriction is decreased (λ increasing).

A. Influence of λ and Reynolds number

The flow rate was calculated by integrating the velocity over a vertical cross section and normalized by the flow rate of a fully open channel (Fig. 2a). The comparison between these results and different orders of the analytical solutions is shown in Fig. 3. For larger δ ($\delta \approx 1$), the zeroth-order analytical solution (CLT) does a poor job of estimating the flow rate, while very good agreement was found between simulation and higher orders of the analytical solution, i.e. the extended lubrication theory provides improvements. The results also indicate that in channels with a high aspect ratio ($\delta = 1$) and at $\mathcal{Re} = 100$, the fourth-order ELT results in about 1% deviation from the numerical analysis while CLT and the second-order ELT deviate about 25% and 5% from the simulation results, respectively.

Contrary to the governing equations used for obtaining the numerical results, the dimensionless governing equations (3) provided for ELT are independent of \mathcal{Re} . Therefore, numerical simulation may help to determine how high the Reynolds number can be in order for the theory to estimate the flow rate accurately. We conducted simulations for \mathcal{Re} up to 2000, and only for channels with a high aspect ratio ($\delta \approx 1$) and a medium gap ($\lambda \approx 0.50$), was the difference between theoretical and numerical results noticeable.

B. Negative shape functions

We consider the initial shape function (10) with λ varying from -1 to 1 (Fig. 4a). We refer to the channel as having a negative shape function if $\lambda < 0$. Since the parametric shape function is the same as in Equation (10), the pressure drop across the channel at different orders can be calculated from Equations (11), (20), and (29) considering $\lambda < 0$. We also conducted numerical simulations for a channel with negative and positive shape functions, $\mathcal{Re} = 100$, and $\delta = 0.1 - 1$. As shown in Fig. 4b, the differences between simulation results and any order of the analytical solutions are within 1% for long channels ($\delta = 0.1$ or less); however, for channels with high aspect ratio, flow rates estimated using CLT, the second-order ELT, and the fourth-order ELT differ about 50%, 17%, and 4% from the simulation results, respectively. These results confirm that higher-order analytical solutions are required to estimate the fluid flow accurately for channels with a negative shape function on the order of the channel height.

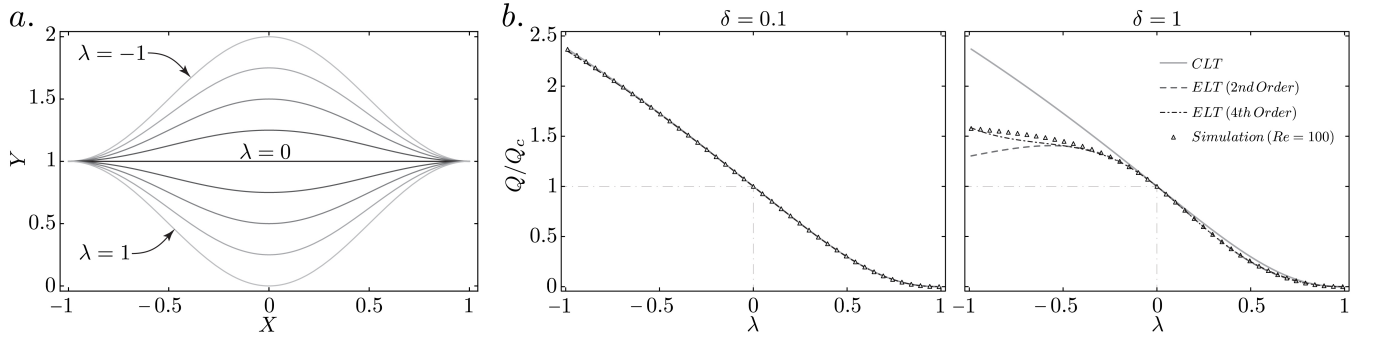


FIG. 4. (a) Cosine shape function (10) with positive and negative λ values. (b,c) Comparison of simulation and analytical results for a channel with a shape function provided in (a) for (b) $\delta = 0.1$ and (c) $\delta = 1$.

IV. PIECE-WISE DIFFERENTIABLE SHAPE FUNCTIONS

We demonstrated that ELT is applicable to a channel with a shape function that is entirely differentiable. This condition may not be met in all applications. Here we provide of an example showing that ELT can be applied for a channel whose shape is continuous and piece-wise differentiable, i.e. the shape function may have non-differentiable points. A channel with such a shape function can be divided into smaller pieces where each part has a differentiable shape. The pressure drop within each piece is estimated using ELT. Since the flow is laminar, the total pressure drop across the original channel is the summation of the pressure drops from all of the pieces. The flow rate is then calculated from the total pressure drop following the procedure mentioned earlier. For example, consider a shape function with a single non-differentiable point as follows

$$H(X) = \begin{cases} 1 - \frac{\lambda}{2\gamma}(X+1) & -1 \leq X \leq 2\gamma - 1, \\ 1 + \frac{\lambda}{2(1-\gamma)}(X-1) & 2\gamma - 1 < X \leq 1, \end{cases} \quad (31)$$

where $0 < \gamma < 1$ is a dimensionless parameter that determines the location of the non-differentiability and $1 - \lambda$ gives the minimum gap height. This shape function is plotted for $\gamma = 0.75$ in Fig. 5a.

We used this same shape function to perform numerical simulations, and the comparison is shown in Fig. 5b. For channels with $\delta = 0.1$ or less, theoretical and numerical results were in good agreement, while for channels with $\delta \approx 1$, flow rates estimated using the higher orders of the analytical solutions more accurately capture the numerical simulations. These results show that ELT can be applied to a channel with a piece-wise differentiable shape function. We note that shape functions can appear on both sides of a channel and the same procedure can be followed to find analytical solutions at different orders.

V. CONCLUSIONS

We extended the lubrication approximation by obtaining higher-order terms in a systematic analysis and verified the analytical results using numerical simulations. Very good agreement was found between higher-order analytical

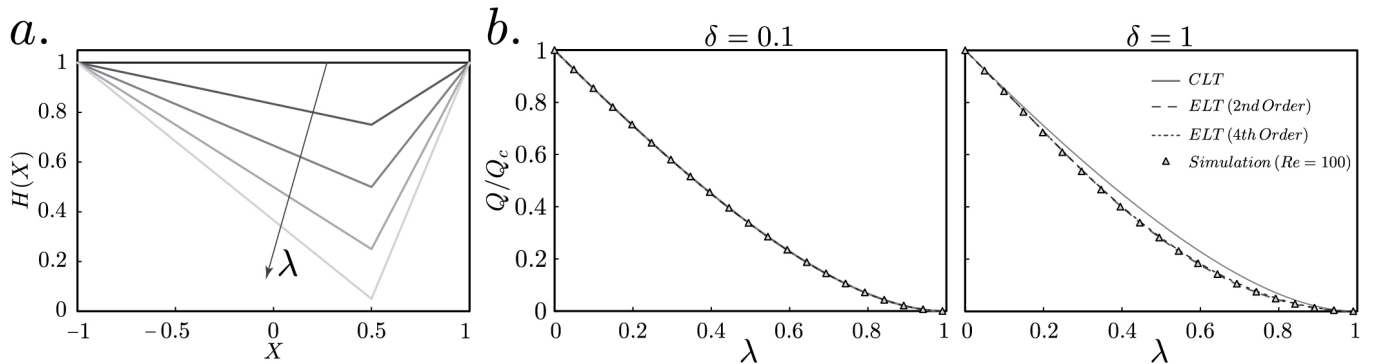


FIG. 5. (a) A piece-wise differentiable shape function as defined in (31) when $\gamma = 0.75$. (b, c) Comparison of simulation and analytical results for the provided shape function for (b) $\delta = 0.1$ and (c) $\delta = 1$.

solutions and the simulation results, which confirms that for channels with a high aspect ratio, the fourth-order extended lubrication theory results in a significant improvement in accuracy as compared to classical lubrication theory. Any piece-wise differentiable shape function can be used with the analytical solutions obtained in this study, which provides a robust tool to estimate the accurately fluid flow in a channel with positive or negative constrictions, whose changes in height are comparable to its length.

VI. APPENDIX. WEAK FORM OF THE CONTINUITY AND NAVIER-STOKES EQUATIONS

We consider an arbitrary pair of P and $\mathbf{U} = (U, V)$ to be a solution to the dimensionless continuity and Navier-Stokes equations (30) for a steady and incompressible flow. If these equations are multiplied by any pressure and velocity basis functions, i.e. (q, ν_1, ν_2) , and integrated over the domain Ω , the pair is still a solution, and satisfies the new equations

$$\begin{aligned} 0 &= \int_{\Omega} \left[\frac{\partial U}{\partial X} + \frac{\partial V}{\partial Y} \right] q \, d\Omega \\ 0 &= \int_{\Omega} \left[\mathcal{Re} \delta \left(U \frac{\partial U}{\partial X} + V \frac{\partial U}{\partial Y} \right) + \frac{\partial P}{\partial X} - \delta^2 \frac{\partial^2 U}{\partial X^2} - \frac{\partial^2 U}{\partial Y^2} - F_x \right] \nu_1 \, d\Omega \\ 0 &= \int_{\Omega} \left[\mathcal{Re} \delta^3 \left(U \frac{\partial V}{\partial X} + V \frac{\partial V}{\partial Y} \right) + \frac{\partial P}{\partial Y} - \delta^4 \frac{\partial^2 V}{\partial X^2} - \delta^2 \frac{\partial^2 V}{\partial Y^2} - F_y \right] \nu_2 \, d\Omega. \end{aligned} \quad (32)$$

We reduce the second-order terms to first-order ones in the above equations by applying Gauss' theorem. For instance, we have

$$\int_{\Omega} \frac{\partial^2 U}{\partial X^2} \nu_1 \, d\Omega = - \int_{\Omega} \frac{\partial U}{\partial X} \frac{\partial \nu_1}{\partial X} \, d\Omega + \int_{\Sigma\Gamma} \frac{\partial U}{\partial X} \nu_1 \, d\Gamma, \quad (33)$$

where Γ is a boundary of Ω , and the last term represents the boundary integrals over all boundaries $\Sigma\Gamma$, which is usually handled separately in finite element packages. After reducing all second-order terms and separating the boundary terms, the weak form of the continuity and Navier-Stokes equations are

$$\begin{aligned} 0 &= \int_{\Omega} \left[\frac{\partial U}{\partial X} + \frac{\partial V}{\partial Y} \right] q \, d\Omega \\ 0 &= \int_{\Omega} \left[\nu_1 \left(\mathcal{Re} \delta \left(U \frac{\partial U}{\partial X} + V \frac{\partial U}{\partial Y} \right) + \frac{\partial P}{\partial X} \right) + \delta^2 \frac{\partial \nu_1}{\partial X} \frac{\partial U}{\partial X} + \frac{\partial \nu_1}{\partial Y} \frac{\partial U}{\partial Y} \right] d\Omega \\ 0 &= \int_{\Omega} \left[\nu_2 \left(\mathcal{Re} \delta^3 \left(U \frac{\partial V}{\partial X} + V \frac{\partial V}{\partial Y} \right) + \frac{\partial P}{\partial Y} \right) + \delta^4 \frac{\partial \nu_2}{\partial X} \frac{\partial V}{\partial X} + \delta^2 \frac{\partial \nu_2}{\partial Y} \frac{\partial V}{\partial Y} \right] d\Omega \end{aligned} \quad (34)$$

-
- [1] W. E. Langlois, *Slow Viscous Flow* (Macmillan, New York, 1964).
 - [2] L. G. Leal, *Advanced Transport Phenomena: Fluid Mechanics and Convective Transport Processes* (Cambridge University Press, Cambridge, 2007).
 - [3] H. Ockendon and J. R. Ockendon, *Viscous Flow* (Cambridge University Press, Cambridge, 1995).
 - [4] A. Szeri, *Fluid Film Lubrication: Theory and Design* (Cambridge University Press, 2005).
 - [5] A. T. John, "Hydrodynamic lubrication," in *Handbook of Lubrication and Tribology, Volume II* (CRC Press, 2012) pp. 1–14, doi:10.1201/b12265-18.
 - [6] H. A. Stone, *Chemical Engineering Science* **60**, 4838 (2005).
 - [7] M. C. Marchetti, J. F. Joanny, S. Ramaswamy, T. B. Liverpool, J. Prost, M. Rao, and R. A. Simha, *Reviews of Modern Physics* **85**, 1143 (2013), rMP.
 - [8] O. Amyot and F. Plouraboué, *Physics of Fluids* **19** (2007).
 - [9] H. A. Stone, A. D. Stroock, and A. Ajdari, *Annual Review of Fluid Mechanics* **36**, 381 (2004).
 - [10] F. Plouraboué, S. Geoffroy, and M. Prat, *Physics of Fluids* **16**, 615 (2004).
 - [11] D. P. Holmes, B. Tavakol, G. Froehlicher, and H. A. Stone, *Soft Matter* **9**, 7049 (2013).
 - [12] Y. Aboelkassem and A. E. Staples, *Acta Mechanica* **223**, 463 (2012).
 - [13] Y. Aboelkassem and A. E. Staples, *Journal of Fluids and Structures* **42**, 187 (2013).
 - [14] J. H. Snoeijer, *Physics of Fluids* **18** (2006).
 - [15] D. Bonn, J. Eggers, J. Indekeu, J. Meunier, and E. Rolley, *Reviews of Modern Physics* **81**, 739 (2009).
 - [16] L. Limat and H. A. Stone, *EPL (Europhysics Letters)* **65**, 365 (2004).